

NRC Publications Archive Archives des publications du CNRC

Durable coronary artery phantoms for optical coherence tomography

Bisaillon, Charles-Étienne; Lanthier, Marie-Michèle; Dufour, Marc;
Lamouche, Guy

This publication could be one of several versions: author's original, accepted manuscript or the publisher's version. /
La version de cette publication peut être l'une des suivantes : la version prépublication de l'auteur, la version
acceptée du manuscrit ou la version de l'éditeur.

For the publisher's version, please access the DOI link below. / Pour consulter la version de l'éditeur, utilisez le lien
DOI ci-dessous.

Publisher's version / Version de l'éditeur:

<https://doi.org/10.1117/12.809086>

Photonic Therapeutics and Diagnostics V, pp. 71612E-1-71612E-10, 2009

NRC Publications Archive Record / Notice des Archives des publications du CNRC :

<https://nrc-publications.canada.ca/eng/view/object/?id=e1dae7fc-a208-4abb-b1cd-df8d980b6054>

<https://publications-cnrc.canada.ca/fra/voir/objet/?id=e1dae7fc-a208-4abb-b1cd-df8d980b6054>

Access and use of this website and the material on it are subject to the Terms and Conditions set forth at

<https://nrc-publications.canada.ca/eng/copyright>

READ THESE TERMS AND CONDITIONS CAREFULLY BEFORE USING THIS WEBSITE.

L'accès à ce site Web et l'utilisation de son contenu sont assujettis aux conditions présentées dans le site

<https://publications-cnrc.canada.ca/fra/droits>

LISEZ CES CONDITIONS ATTENTIVEMENT AVANT D'UTILISER CE SITE WEB.

Questions? Contact the NRC Publications Archive team at

PublicationsArchive-ArchivesPublications@nrc-cnrc.gc.ca. If you wish to email the authors directly, please see the
first page of the publication for their contact information.

Vous avez des questions? Nous pouvons vous aider. Pour communiquer directement avec un auteur, consultez la
première page de la revue dans laquelle son article a été publié afin de trouver ses coordonnées. Si vous n'arrivez
pas à les repérer, communiquez avec nous à PublicationsArchive-ArchivesPublications@nrc-cnrc.gc.ca.

Durable coronary artery phantoms for optical coherence tomography

Charles-Étienne Bisaiillon^a, Marie-Michèle Lanthier^{a,b},
Marc L. Dufour^a, Guy Lamouche^{a,b}

^a Industrial Materials Institute, National Research Council Canada, Boucherville

^b Engineering Physics Department, Ecole Polytechnique de Montréal

ABSTRACT

We developed coronary artery phantoms that should be of great use for intravascular optical coherence tomography. Our phantoms mimic the OCT signal profile of coronary arteries, show mechanical properties approaching those of real tissue, and are durable.

Keywords: Optical coherence tomography, phantoms, coronary arteries

1. INTRODUCTION

Recent progress achieved in using optical coherence tomography (OCT) to image coronary arteries show that this technique is becoming a powerful diagnostic tool in cardiology. OCT systems have typical resolutions ranging from 5 to 20 μm . By guiding light through catheterized probes, the coronary arteries can be reached to acquire detailed and contrasted images of the artery wall in-vivo. Therefore, OCT can be used as a diagnostic tool to detect atherosclerosis and assess the vulnerability of plaque. It can also be used as a post-treatment tool to verify stent apposition. The development of such systems involves many challenges. In overcoming these challenges, the potential uses for stable optical phantoms mimicking arteries are numerous. These can be used to assess the good functionality of OCT systems and catheterized probes. They can be used as a calibration tool to insure repeatability of measurement. Images obtained from such phantoms are also useful for testing new image processing techniques.

In this paper, we present a technique for the fabrication of durable artery phantoms. Our approach enables the reproduction of a wide range of optical properties found in coronary arteries as well as their mechanical properties. By adding several layers of carefully prepared mixtures one over the other, we reproduce the morphology of sound arteries and eventually aim at replicating other features such as plaque.

In section 2, we present the methodology for the replication of the various properties of the arteries. In section 3, we describe the experimental results that led to the determination of the phantoms optical characteristics. In section 4, we present some mechanical properties of the phantoms. In section 5, we illustrate the utility of the phantoms through several examples. In section 6, we discuss the ongoing developments.

2. METHODOLOGY

2.1 Optical characteristics

Our goal is to design phantoms primarily for OCT, although they could be used for other optical imaging techniques. Figure 1 shows an OCT image of a sound porcine left anterior descending (LAD) artery extracted from the heart. This image was obtained with an OCT system and an intravascular OCT probe developed in our laboratories. Well contrasted layers may be observed. They correspond to the anatomy of a sound coronary artery: the very thin intima delimiting the lumen, the media and the adventitia. Mimicking that particular optical signature is our main objective. We also aim at developing a technique to fabricate phantoms that are durable and reproducible.

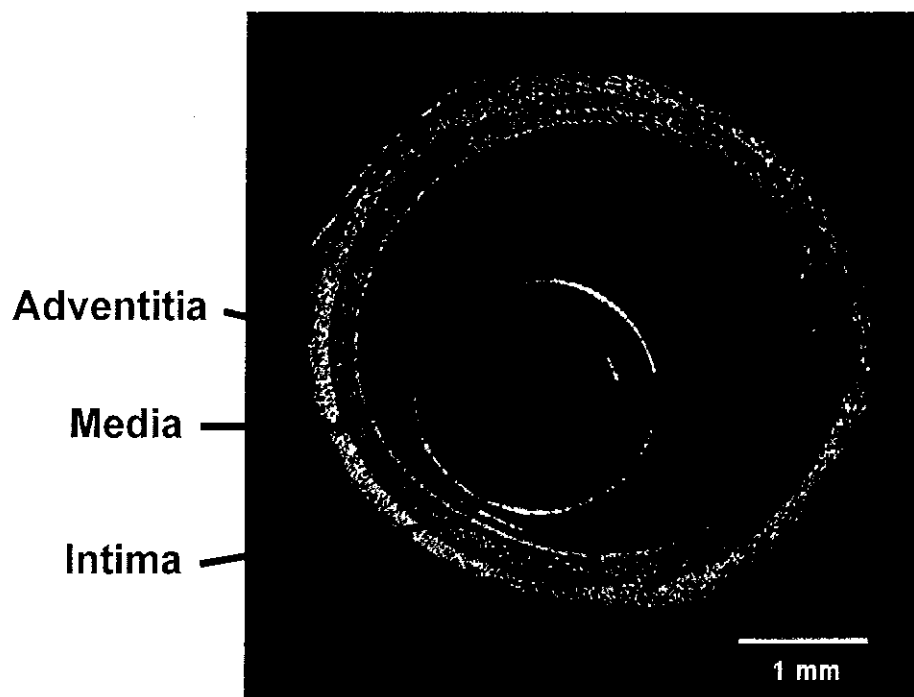


Fig. 1: OCT image of a sound porcine coronary artery.

In this first attempt at creating phantoms, the layers of healthy arteries are considered homogeneous. In a homogeneous scattering medium, the amplitude of the OCT signal is related to the backscattering and decays with the total attenuation. Therefore, we need to obtain the values of the backscattering amplitude and the total attenuation for each layer of the tissue. This asks for the creation of three mixtures that match these properties and that can be crafted in layered tubular phantoms.

Required optical properties are obtained by mixing known concentrations of a scattering powder and of an absorbing material in a transparent matrix. The scattering amplitude of the OCT signal can be related to the concentration of the powder. In a previous paper, we detailed a model showing that the amplitude of the OCT signal is proportional to the square root of the concentration of particles [1]. For the attenuation, the impact of every particle is additive, and therefore, it is proportional to the concentration of the powder. The scattering powder alone does not attenuate the OCT signal as much as what is observed in the artery tissue. The desired attenuation is obtained by adding an absorbing material.

2.2 Fabrication

The matrix of the phantoms is a mixture of Sylgard 184 silicone and of pure (poly)dimethylsiloxane (PDMS, Dow Corning 200R, 50 cSt viscosity). Both compounds are inorganic. They come in liquid form but cure together with the action of a reactive component and heat. After curing, they are highly stable, yielding phantoms with a very long life. The Sylgard 184 is sold in a kit of resin and reactive to typically be mixed in a 10:1, resin:reactive ratio. However, the variation of that ratio and the addition of pure PDMS allow great variation of the elasticity after curing [2, 3]. The cured matrix is transparent, weakly absorptive at 1.3 μm and has a group refractive index around 1.4. It is also quite practical to work with.

The scattering is obtained by the addition of alumina powder. A 1 μm grade de-agglomerated polishing powder was kindly provided by Struers. Scanning electron microscopy (SEM) of a sample showed that most particles are smaller than 0.3 μm . The refractive index of alumina is 1.76 and its specific gravity is 3.97 g/cm^3 .

Although the alumina itself provides some attenuation, another material is needed to avoid being limited to the combination of scattering – attenuation related to the alumina concentrations. An ideal product would be an absolute absorptive material (meaning one that does not scatter). However, rare are the transparent chemicals that can absorb as much as water at 1.3 μm and that are soluble in silicone. We tried china ink, which is often considered as an absolute absorbent. However, the silicone matrix is highly hydrophobic and a uniform mixture could not be obtained. Attempts at drying out the ink and dispersing it again in the silicone were unsuccessful because the ink binds strongly out of solution. We then decided that coloring our mixture in black could be an adequate solution and we tried incorporating a 6 μm graphite powder. It proved to absorb light very well at 1.3 μm but the 6 μm particles were too large compared to the OCT resolution to obtain the desired uniformity. Finally, we tried carbon black powder (Monarch 700, kindly provided by the Powder Forming group at IMI) because it has the same composition but with a smaller particle size. We obtained strong attenuation and good uniformity. Although we measured some small scattering from carbon black in OCT images, it showed to be weak enough to consider the product as a pure absorbent.

Phantoms with the desired optical and mechanical properties are then made by weighing the needed amount of each powder and by adding the Sylgard 184 and the pure PDMS in necessary volumes. Ultrasonic bathing is used to insure a uniform dispersion of the particles. To create the coronary artery phantoms in particular, different mixtures reproducing the distinct properties of each anatomical layer are prepared. The mixtures are successively applied and cured on a lathe close to a heating element. The setup is showed in Fig. 2.

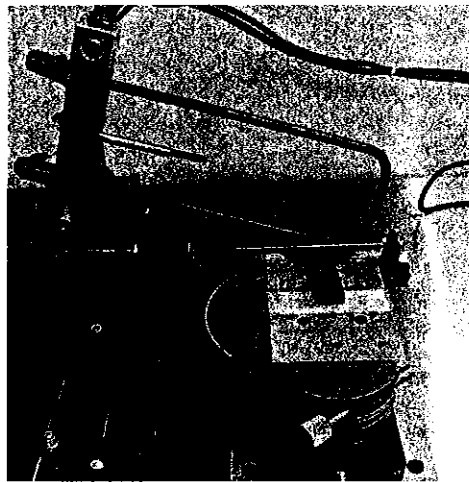


Fig. 2 : Lathe setup for multilayer phantom fabrication.

3. OPTICAL PROPERTIES

3.1 Artery signal

The phantom design process starts with the quantification of the scattering and of the total attenuation of the OCT signal for each biological tissue we wish to replicate. To develop the technique, we focus primarily on sound coronary arteries, seeking to obtain representative values for the properties. These values are obtained by imaging a sample of porcine artery, extracted and cut flat open, in a bench top configuration. The images are then analyzed by treating each layer as a homogeneous medium. In each image, the amplitude of the OCT signal ($\langle S_{OCT} \rangle$) along the depth is averaged over regions where the layers have even thicknesses. The resulting average profiles are then fitted for each layer with a model of exponential decay:

$$\langle S_{OCT} \rangle \propto A \exp \left[-2\alpha \frac{z - z_0}{n} \right] \quad (\text{Eq. 1})$$

where z is the optical depth in the image and z_0 is the depth of the starting edge of a layer in the profile. The decay parameter α corresponds to the total attenuation of the electric field. The parameter n is the refractive index. It is used to convert optical depths to geometrical depths. The factor 2 in the equation accounts for the light being reflected back in

the system. The parameter A corresponds to the backscattered amplitude. It is corrected for the accumulated attenuation. It is also corrected for both the focusing and collecting parts of the beam propagation. These corrections are not explicitly shown in Eq. 1. The values of A will be given in units relative to the system. By making the phantoms to match the values of α and A when measured in the same configuration, we can obtain matching backscattering and attenuation. The whole process is illustrated at Fig. 3, where an OCT image is shown on the left and its average profile is aligned on the right with the fitted curves plotted over it. The values for the fitting parameters given in Fig. 3 are averaged values obtained from a few images of a single sample. Those are our targeted characteristics. Note that the intima being so thin, its attenuation can be neglected.

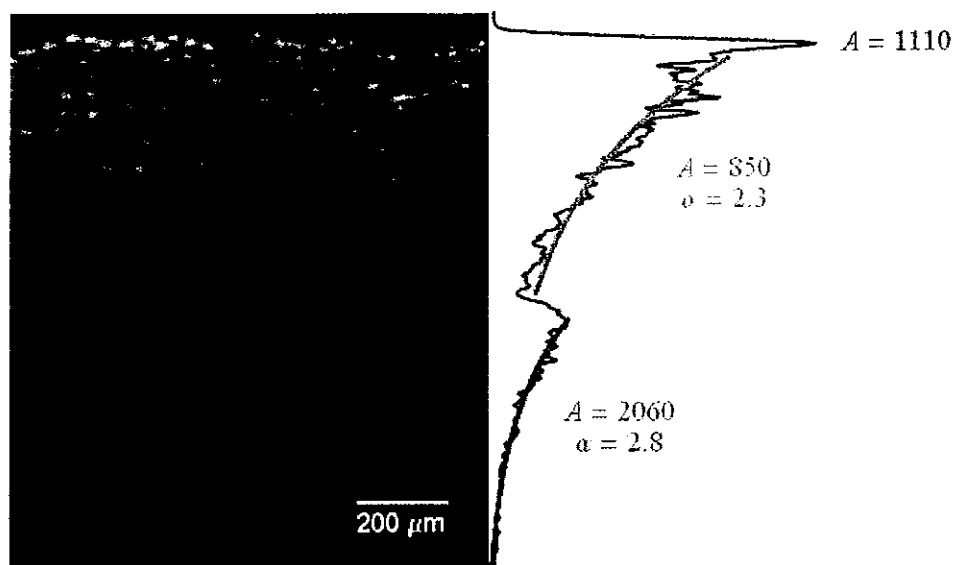


Fig. 3: OCT image of a porcine coronary artery and its average profile fitted for the amplitude and the total attenuation of the three layers.

3.2 Phantom signal

The second step of the design process of our phantoms is to evaluate how the OCT signal amplitude and its total attenuation vary with the concentrations of alumina and carbon black in silicone. This will determine the concentrations required for each layer. The properties were obtained by fitting OCT image profiles in the same manner as for the artery.

To characterize the alumina-silicone combination, twelve disc-shape phantoms with alumina concentrations ranging from 1 to 36 mg/ml were produced and imaged in the same bench top configuration as the artery sample. The scattering amplitude and total attenuation coefficients obtained by fitting the profiles are plotted in Fig. 4 and Fig. 5. In Fig. 4, we observe a good agreement between the data and the expected square-root model. This highlights the uniformity of samples that is obtained from the mixing technique. In Fig. 5, there is also very good agreement of the variation of the attenuation to the concentration with the expected linear relationship for low concentrations. The exact nature for the deviation observed at high concentrations is currently investigated.

Since we consider that the alumina is the main scatterer, the concentrations needed to obtain the scattering amplitude in each layer mixture are deduced from Fig. 4. To mimic the scattering properties of the intima, the media and the adventitia, concentrations of 15 mg/ml, 10 mg/ml and 35 mg/ml are good approximations. These concentrations, however, create a certain attenuation of the signal that can't be neglected. The corresponding attenuation coefficients are found by referring to Fig. 5. The attenuation from the intima is already neglected since the layer is very thin. For the adventitia, we consider that the attenuation caused by the 35 mg/ml is close enough to the actual layer value. For the media, the 1.0 mm^{-1} total attenuation from 10 mg/ml alumina in silicone does not match the 2.3 mm^{-1} measured on the artery sample. This discrepancy can be solved by adding carbon black to the phantom.

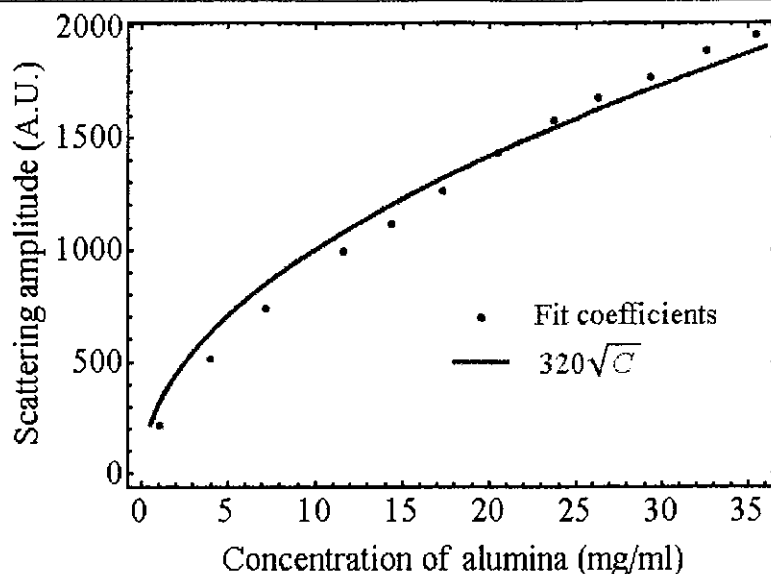


Fig. 4: Fitted amplitude coefficients vs alumina concentration and related square root model.

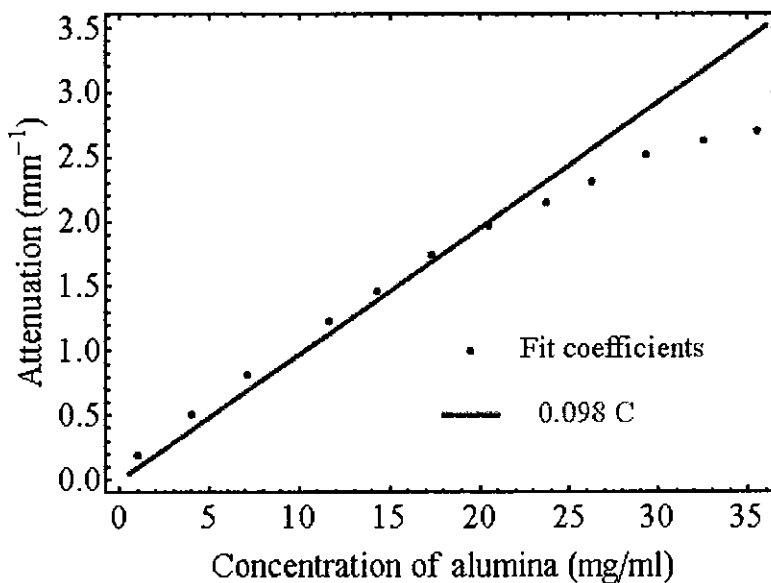


Fig. 5: Fitted attenuation coefficients vs alumina concentration and linear model.

To characterize the carbon black in silicone combination, we produced eight disc-shape phantoms with concentrations of carbon black ranging from 0.2 to 1.6 mg/ml. Although the scattering from carbon black is weak compared to that from alumina, there is still enough amplitude to measure the attenuation coefficients from the OCT signal profiles. This was done in the same manner as for the artery and the alumina phantoms. The measured attenuation coefficients are plotted in Fig. 6. A good linear relationship between the coefficients and the concentration of carbon black is observed. As estimated from Fig. 6, the concentration of carbon black needed in the media mixture is set to 0.5 mg/ml.

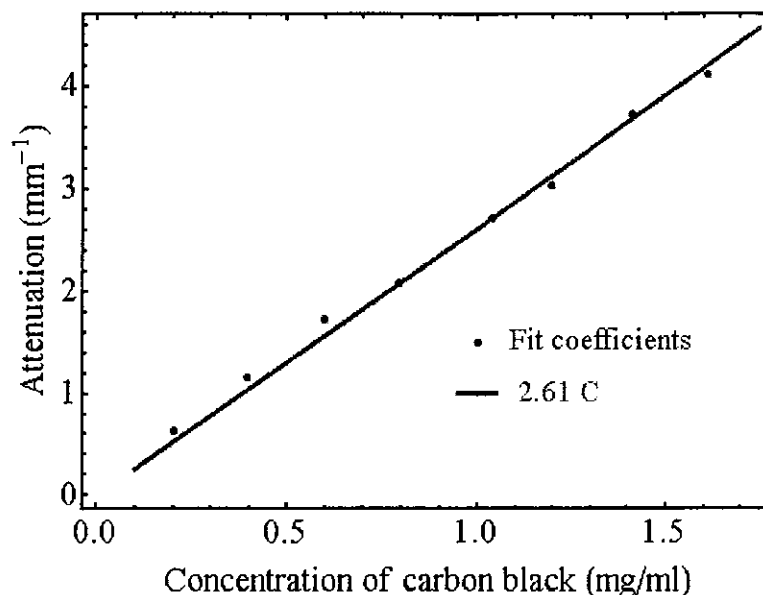


Fig. 6: Fitted attenuation coefficients vs carbon black concentration and a linear model.

3.3 Artery phantom

Once the three mixtures previously described are prepared, the artery phantoms are crafted. Fig. 7 shows a picture of two phantoms. The phantoms both have a 3 mm diameter lumen but different wall thicknesses. The layers are very obvious in the cross-sectional view. The first layer made from a mixture of only alumina and silicone appears as a thin white line and is used to represent the intima. It is followed by the media which appears dark gray since it also contains carbon black. Finally at the outer border is the white layer with alumina mimicking the adventitia.

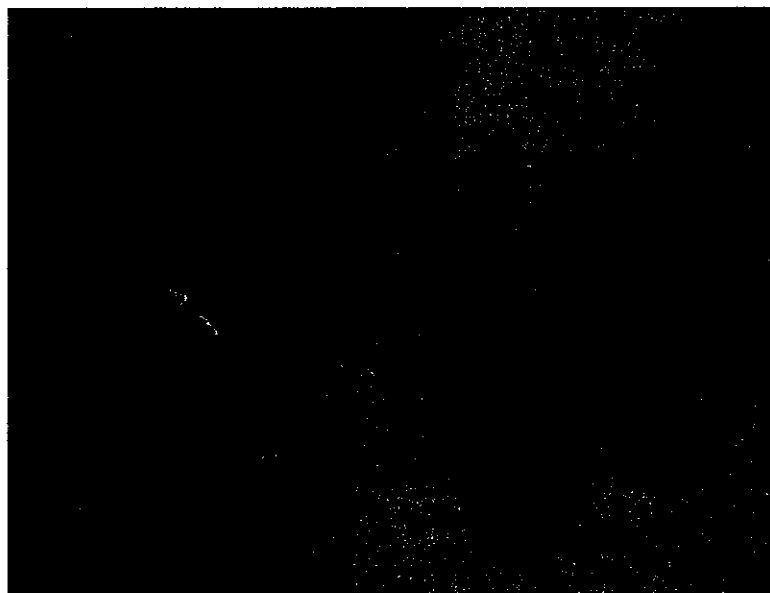


Fig. 7: Photo of two sound coronary artery phantoms crafted with different layer thickness.

The result of an OCT image acquired with our catheterized imaging system is presented at Fig. 8. The three-layer characteristic signal of a sound coronary artery is very obvious. We can also observe reflections from the guiding catheter that contains the rotating probe and from the inflation balloon (upper left region) used to flush blood in clinical situations.

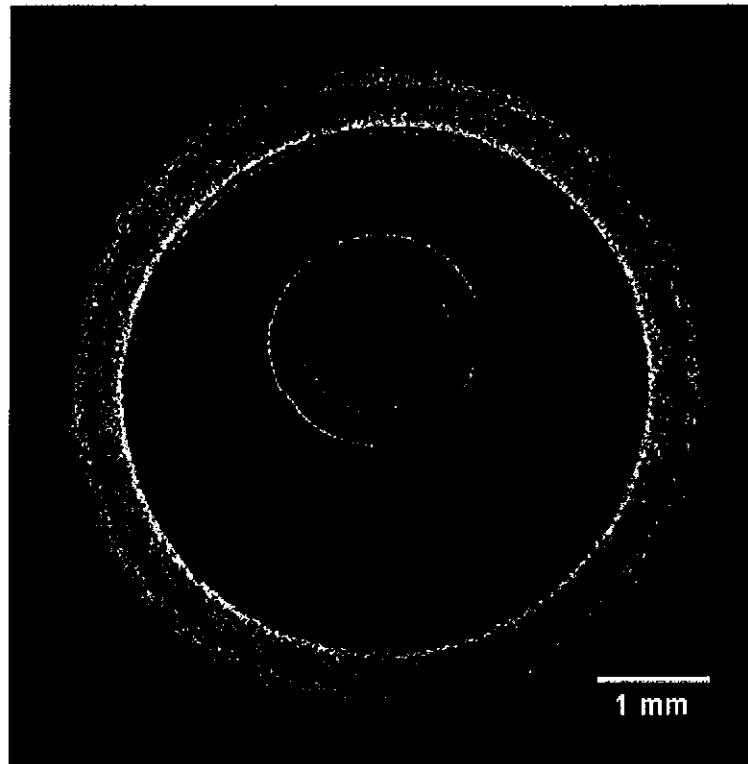


Fig. 8: Time domain OCT image of a coronary artery phantom.

4. MECHANICAL CHARACTERIZATION

The elasticity of the phantoms was evaluated by performing uniaxial traction tests on blank samples of silicone with various combinations of PDMS, Sylgard resin, and Sylgard reactive (Sylgard 184). Results from these experiments are compared to data obtained on porcine tissues in Fig. 9.

We can observe that there is a decrease in stiffness with the increase of the resin to reactive ratio of Sylgard 184. However, a ratio higher than 15:1 does not further decrease the stiffness and leads to very sticky samples while still being quite stiffer than soft tissues. A further decrease in stiffness can be obtained by the addition of pure PDMS. Mixtures containing PDMS no longer cure at room temperature, but do polymerize within one to two hours at a higher temperature. According to the results in Fig. 9, a proportion of 22.5:15:1 of PDMS:Sylgard Resin:Sylgard Reactive can produce samples as soft as coronary arteries in their linear regime. However, the phantoms produced yet have ratios up to 15:15:1 because they are easier to remove from the lathe shaft.

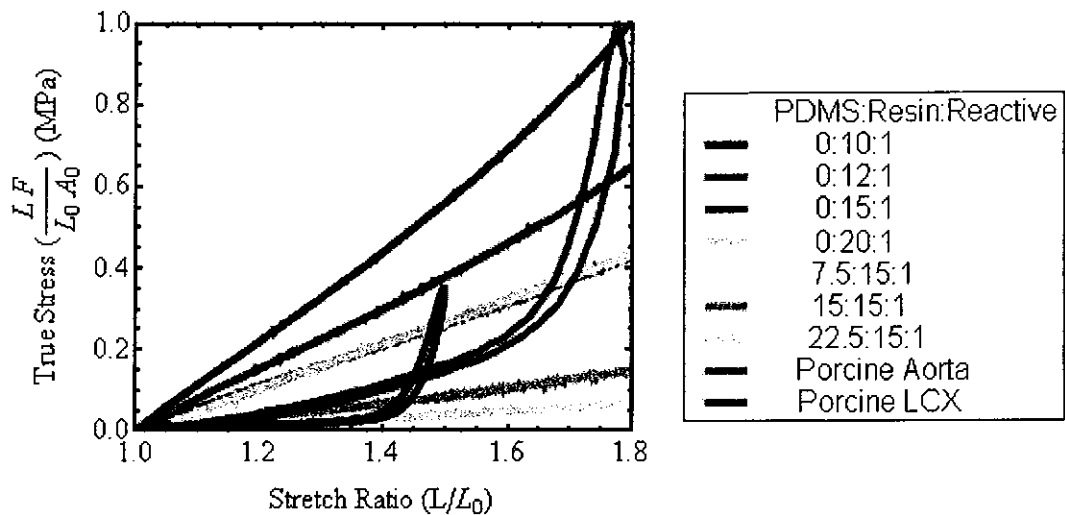


Fig. 9 : Elasticity of different compositions of silicone compared to porcine aorta and a porcine left circumflex artery (LCX).

5. APPLICATIONS

The first incentive for developing these phantoms was our own needs related to the development of intravascular OCT systems, both time-domain OCT and swept-source OCT, and of catheterized probes. The phantoms revealed to be an invaluable asset for many aspects of this work. Unlike arteries, they are always available and their properties are stable and reproducible. In many contexts, like after performing hardware and software modifications or after moving the systems from one location to another, the phantoms are used to quickly verify the good operation of the system. They are also often used before measurement on arteries to optimize the image quality since they provide a signal very similar to that of the arteries.

Besides these practical advantages, the phantoms are found particularly useful in developing image processing techniques. For example, Fig. 10 shows an image of a phantom with its internal and external boundaries emphasized. The algorithm used relies on a few consecutive A-scans to detect the boundaries in real time. The algorithm comes from a modified version of a boundary detection algorithm described first by Koozekanani [4]. The process involves filtration, zero crossing detection, weighing pixels, and interpolation between a few successive A-scans.

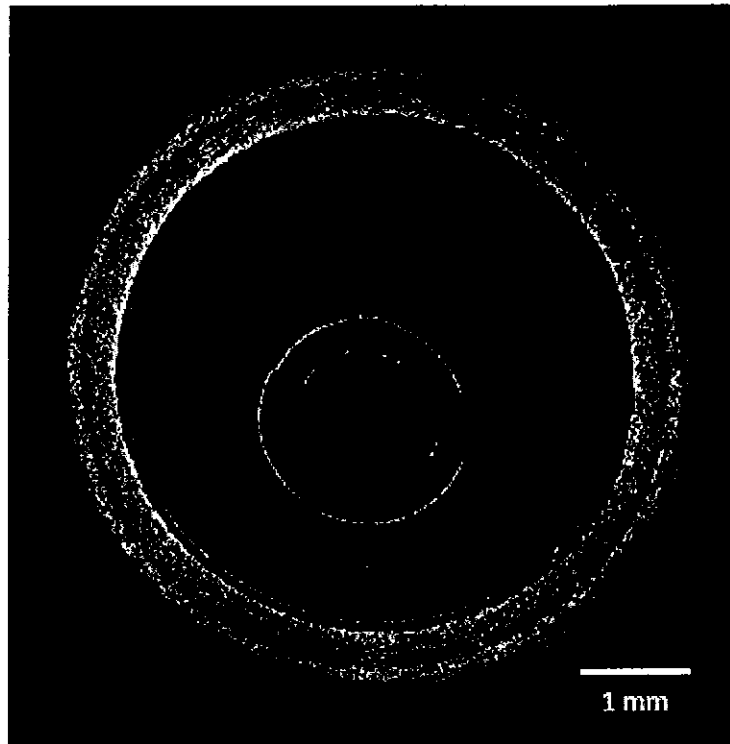


Fig. 10: OCT image of an artery phantom, with the lumen and external edge emphasized.

The phantoms are of great value for testing such algorithms. They can be fabricated with a wide range of optical properties and with different shapes. Consequently, some phantoms can be fabricated with specific properties to test the limits of such segmentation algorithms. The durability of the phantoms is also of importance. Different versions of an algorithm can be tested from measurements performed on the same phantom at different times or using different systems.

6. FURTHER DEVELOPMENTS

In this paper, our goal was to develop a technique to produce artery phantom. Since the fabrication process was our main focus, we worked on mimicking the optical properties of a single artery. The next step is to use a more representative and refined model of the sound artery based on measurements performed on a large number of samples.

In the near future, we wish to produce phantoms of diseased arteries. The first step will be to collect data on the scattering and the total attenuation from features like lipid pools, calcified plaques, etc. With the versatility allowed by our technique, mimicking the properties of most of these features should not cause too many problems. The biggest challenge may reside in crafting the morphology of these diseased artery phantoms.

The technique we developed also enables the tuning of the mechanical properties. We demonstrated previously that a wide range of elasticity, including the elastic regime of arteries, is accessible with the PDMS and Sylgard 184 combination. However, the nonlinear strain hardening characteristic of tissues is not obtained at the same order of deformation. Improving the mechanical behavior may lead us to try other matrix formulations or materials.

7. CONCLUSION

In summary, we presented a technique to fabricate multilayered cylindrical phantoms from various combinations of PDMS and Sylgard 184 as the matrix, of aluminum oxide as the scatterer, and of carbon black as the absorbent. The resulting phantoms can replicate the OCT signal of sound coronary arteries while having similar elasticity. These phantoms are very useful in the development of OCT intravascular technology. In a near future, we plan to refine our optical characterization of arteries, to imitate complex features, and to improve the mechanical behavior of the phantoms.

8. REFERENCES

- [1] Bisailon, C.-E., Lamouche, G., Maciejko, R., Dufour, M. and Monchalain, J.-P., "Deformable and durable phantoms with controlled density of scatterers," *Physics in Medicine and Biology* **53**(13), N237-N247 (2008)
- [2] Oldenburg, A. L., Touban, F. J.-J., Suslick, K. S., Wei, A. and Boppart, S. A., "Magnetomotive contrast for in vivo optical coherence tomography," *OPTICS EXPRESS* **13**(17), 6597-6614 (2005)
- [3] Jiang, S., Pogue, B. W., McBride, T. O. and Doyley, M. M., "Near-infrared breast tomography calibration with optoelastic tissue simulating phantoms," *Journal of electronic imaging* **12**(4), 613-620 (2003)
- [4] Koozekanani, D., Boyer, K. and Roberts, C., "Retinal thickness measurements from optical coherence tomography using a Markov boundary model," *Medical Imaging, IEEE Transactions on* **20**(9), 900-916 (2001)